2009

Physiological responses of red mangroves to the climate in the Florida Everglades

Jordan G. Barr
Department of Environmental Sciences, University of Virginia and Everglades National Park

Jose D. Fuentes
Department of Environmental Sciences, University of Virginia

Vic Engel
Everglades National Park

Joseph C. Zieman
Department of Environmental Sciences, University of Virginia

Follow this and additional works at: https://digitalcommons.fiu.edu/fce_lter_journal_articles

Physiological responses of red mangroves to the climate in the Florida Everglades

Jordan G. Barr,[1,2] Jose D. Fuentes,[1] Vic Engel,[2] and Joseph C. Zieman[1]

[1]   This manuscript reports the findings of physiological studies of red mangrove (*Rhizophora mangle L.*) conducted from June to August 2001 and from May to June 2003 in the Florida Everglades. In situ physiological measurements were made using environmentally controlled gas exchange systems. The field investigations were carried out to define how regional climate constrains mangrove physiology and ecosystem carbon assimilation. In addition, maximum carboxylation and photosynthetic active radiation (PAR) limited carbon assimilation capacities were investigated during the summer season to evaluate whether ecophysiological models developed for mesophyte plant species can be applied to mangroves. Under summertime conditions in the Florida Everglades, maximum foliar carbon dioxide (CO_2) assimilation rates reached 18 μmol CO_2 m^{-2} s^{-1}. Peak molar stomatal conductance to water vapor (H_2O) diffusion reached 300 mmol H_2O m^{-2} s^{-1}. Maximum carboxylation and PAR-limited carbon assimilation rates at the foliage temperature of 30°C attained 76.1 ± 23.4 μmol CO_2 m^{-2} s^{-1} and 128.1 ± 32.9 μmol (e^{-}) m^{-2} s^{-1}, respectively. Environmental stressors such as the presence of hypersaline conditions and high solar irradiance loading (>500 W m^{-2} or >1000 μmoles of photons m^{-2} s^{-1} of PAR) imposed sharp reductions in carbon assimilation rates and suppressed stomatal conductance. On the basis of both field observations and model analyses, it is also concluded that existing ecophysiological models need to be modified to consider the influences of hypersaline and high radiational loadings on the physiological responses of red mangroves.

1. Introduction

[2]   Mangroves are found along the coast in tropical regions around the world and exhibit high rates of productivity [*Mitsch and Gosselink*, 2000] and dynamic biogeochemical cycles [*Bouillon et al.*, 2008; *Robertson and Alongi*, 1992; *Twilley et al.*, 1992]. Covering a global extent of $1.7-1.8 \times 10^5$ km^2, mangroves provide numerous ecological services [*Valiela et al.*, 2001]. Mangrove ecosystems are also known to store large amounts of carbon in peat soils (retained by mangrove prop roots), and exhibit complex nutrient dynamics which are regulated, in part, by tidal activity, salinity fluctuations, and upstream water management [*Twilley et al.*, 1992; *Smith et al.*, 1994; *Alongi*, 2008; *Bouillon et al.*, 2008]. Presently, mangroves are under the influence of sea level rise and in some instances (such as in Florida) experience major disturbances created by storm activity [*Smith et al.*, 1994; *Alongi*, 2008].

[3]   Environmental stressors exert a strong influence on the carbon balance and growth form of mangrove species.

[1]Department of Environmental Sciences, University of Virginia, Charlottesville, Virginia, USA.
[2]Everglades National Park, Homestead, Florida, USA.

First, mangrove roots are often inundated with saline waters, creating an osmotic resistance to fresh water uptake. During periods of high evaporative demand, salt-excluding mangrove species need to conserve water because of limited capacity to extract fresh water from saline soils. As a result, water use efficiencies in some mangroves are thought to be among the highest of all C$_3$ plant species [*Ball*, 1986]. High water use efficiency and the energetic costs of excreting and/or excluding salts come at the expense of reduced rates of carbon assimilation [*Ball et al.*, 1988]. Second, mangroves species are tropical plants and their leaves experience exceedingly high (>1000 W m^{-2}) solar irradiance loadings. In saline environments, mangroves must conserve water by reducing transpiration during periods of high evaporative demand. Thus, transpiration cooling at the leaf surface may not be an effective mechanism to protect foliage from excessive heating and inhibition of photosynthesis. The modulation of foliage temperatures may be accomplished instead by changing leaf angles to reduce solar energy interception, decreasing leaf size to augment boundary layer sensible heat transport, or increasing leaf succulence to raise foliage specific heat capacity [*Ball et al.*, 1988]. These types of adaptations are likely to have a significant impact on the carbon uptake of mangrove tree species and on the overall carbon balance of these ecosystems. Increasing our knowledge of diurnal leaf-level fluxes

and physiological responses to environmental conditions in mangrove species will improve understanding of carbon fluxes in these systems.

[4] The mangrove forests of the Florida Everglades, USA, are experiencing rapid environmental changes associated with upstream water management practices along with natural disturbances such as hurricanes, sea level rise, and fluctuating salinity gradients [Smith et al., 1994; Ward et al., 2006]. Environmental regulators operating along conspicuous gradients define mangrove vegetation dynamics and species composition in the Everglades. In the southeastern portion of the Everglades, the dominant species is red mangrove (Rhizophora mangle L.), existing in scrub and dwarf forms and reaching 2.5 m in height. In the southwestern portions of the Everglades and along the fringes of the numerous islands in and around Florida Bay, red mangroves occur in a taller form, reaching 30 m at maturity in dense stands [Lin and Sternberg, 1992a; Lugo and Snedaker, 1974]. The dwarf variants principally inhabit low-nutrient environments with relatively shallow peat soils and high salinity levels [Koch and Snedaker, 1997]. The tall, fringe mangroves are typically found in areas with higher nutrient content and lower salinities compared to the areas inhabited by the dwarf variant.

[5] Here, we investigated diurnal, in situ gas exchange rates on a large number of R. mangle leaves to address three research objectives. Our first objective was to determine the rates of carbon dioxide assimilation (A_N) and stomatal conductance to water vapor (g_{sv}) under different levels of solar irradiance. A subset of these measurements were used to compare diurnal fluxes in leaves subject to direct solar irradiance throughout the day to leaves in the forest interior experiencing sunflecks or partial shading. The second objective was to quantify maximum carboxylation and PAR-limited carbon assimilation capacities so that such physiological attributes can be included in canopy models designed to investigate net carbon ecosystem exchanges. Leaf-level measurements were obtained from 'tall' and 'dwarf' red mangroves to ascertain whether the different morphological characteristics and salinity effects were reflected in A_N and water- and light-use efficiencies. The third goal of this study was to evaluate whether leaf-level models of A_N and g_{sv} developed for mesophyte plant species can be applied to red mangroves. The information on foliage physiological attributes was incorporated into a canopy-scale model to estimate seasonal forest carbon assimilation rates. The modeling effort is part of a larger collaboration with the Florida Coast Everglades Long-term Ecological Research (FCE LTER) program (http://fcelter. fiu.edu), in which we are currently quantifying the land surface-atmosphere net carbon dioxide exchange in an Everglades mangrove forest using eddy covariance fluxes [Barr, 2005].

2. Methods

2.1. Field Sites

[6] Physiological measurements were made in a dense, mature mangrove forest along the shoreline of Key Largo, and along the Taylor River in the coastal Florida Everglades. The Key Largo site (Figure 1) is located on the Florida Keys, with annual precipitation of approximately 750 mm. The canopy height at this site is approximately 10 m. The Taylor River site is in the southern portion of Everglades National Park with annual rainfall typically exceeding 1500 mm, and with seasonal salinity fluctuations ranging from 0 to >35 ‰. In contrast to the Key Largo site, the Taylor River site is characterized by dwarf (~1 m) red mangroves irregularly spaced across the landscape. The Taylor River site is known to experience hypersaline conditions during periods of low rainfall and is also considered to be oligotrophic. Leaf-level measurements were also taken on mangroves at two other sites (the Watson River Chickee and at Little Rabbit Key) and were included in the calculations of leaf model parameters.

2.2. Leaf-Level Gas Exchange

[7] At the Key Largo and Taylor River sites, we measured diurnal changes in leaf carbon assimilation, transpiration, and stomatal conductance to water vapor using a portable gas exchange system (model LI-6400, LiCor Inc., Lincoln, NB). For each measurement, the leaves remained in the LI-6400 cuvette long enough (2–3 min) to obtain 5–10 readings per leaf. Irradiance levels inside the cuvette followed the ambient PAR values, which were measured with an externally mounted quantum sensor. Leaf temperature in the cuvette was maintained to within ±2°C of ambient temperature using the Peltier heating/cooling module. The water vapor pressure deficit (VPD) between the leaf and surrounding air was maintained at <2 kPa. In all experiments, leaves were randomly selected based on the conditions that (1) the leaves must have been within reach either from land or from a boat, and (2) the leaves were not senescing. Therefore, measurements were made on an ensemble of healthy leaves of different ages, but not on leaves near the end of their life cycle.

[8] Two sets of measurements were taken at the Key Largo site. For the first set, we tagged 21 individual leaves on branches reached from the shoreline. Gas exchange rates were measured on each tagged leaf in succession, taking approximately 45 min to cycle through all tagged leaves, and enabling several measurement cycles over the course of the day. These measurements were taken on 26 July, 7 August, and 13 August 2001. An open field lies to the east and south, so the foliage was in direct solar irradiance until 14:00 h. After this time, foliage experienced sunfleck conditions with shade gradually increasing throughout the afternoon as the solar angle declined below the height of a mangrove stand to the west of the study site. A second set of measurements focused on a subset of leaves exposed to direct solar irradiance. These measurements were made on 24 July 2001 and 27 May 2003 using a boat to access sunlit foliage along the shoreline as the solar zenith angle changed. On 24 July and 27 May, a total of 1117 and 1380 observations were made, respectively, representing 220 and 280 individual leaves, respectively. Leaf-level gas exchange measurements at the Taylor River site also focused on foliage that was exposed to direct solar irradiance. The canopy was only ~1 m tall, and the foliage was sparse such that shading inside the canopy was minimal. During 19 July 2001, 19 May 2003, and 4 June 2003, a total of 217, 617, and 1459 observations were made, respectively, representing 40, 120, and 290
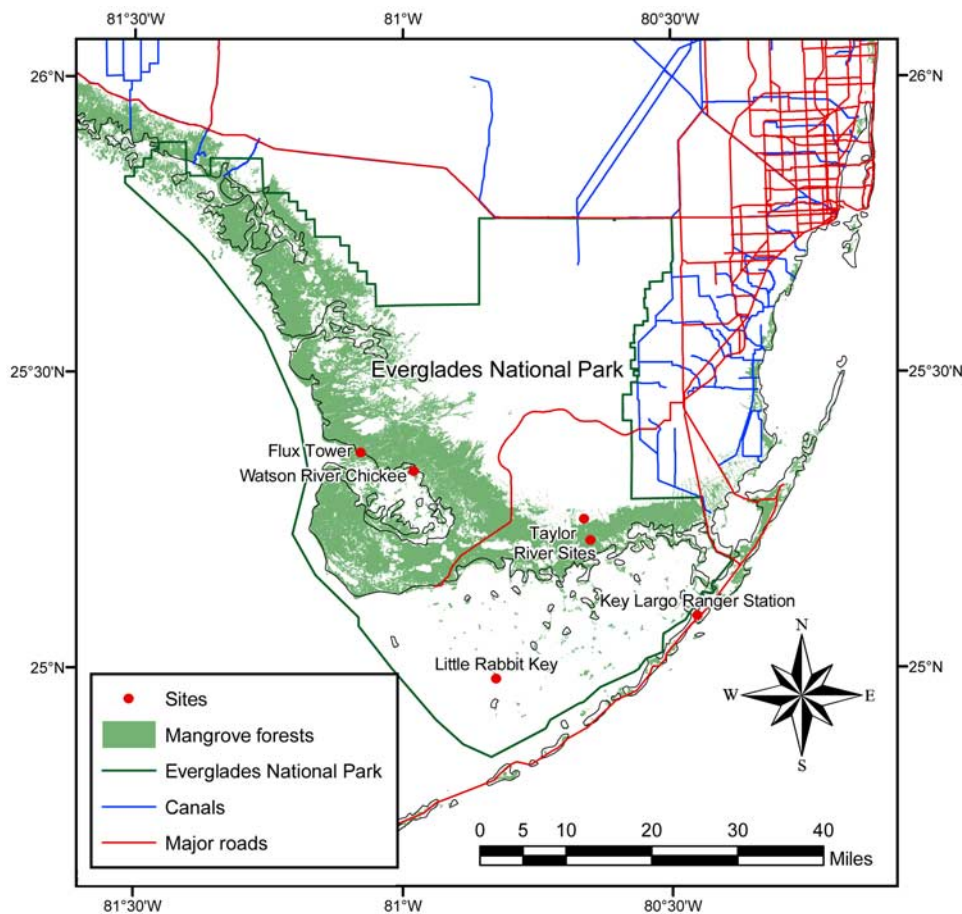
Figure 1. Map of Florida Everglades showing the field sites including Key Largo, Taylor River, Little Rabbit Key, and Watson River Chickee.

individual leaf elements, respectively. The number of measurements was much lower on 19 July because stomatal conductance and intercellular CO_2 mixing ratio quantities stabilized slowly. Ensemble values of A_N and transpiration rates represented in each equally spaced PAR and g_{sv} bin were expressed as one standard deviation from the mean quantities. Cuvette data were also used to calculate leaf-level water use efficiency (WUE) and light use efficiency (LUE) for sunlit leaves on fringe and dwarf mangroves. For this study, WUE is defined as the ratio of A_N to g_{sv}. LUE is defined as the ratio of A_N to the measured PAR incident on the leaf surface. Ensemble average values of A_N, g_{sv}, and PAR were used to generate diurnal patterns of WUE and LUE.

2.3. Leaf-Level Models

[9] A central goal of this research is to evaluate whether leaf-level models of A_N and g_{sv} developed for mesophyte plant species can be applied to red mangroves. To accomplish this goal, we used a traditional Michaelis-type model (equation (1)) to represent photosynthetic responses to intercepted PAR. This model is frequently used for terrestrial species [e.g., *Dwyer and Stewart*, 1986; *Fuentes and King*, 1989; *Wilson et al.*, 2000]. We used multivariate linear regression to obtain estimates of the apparent quantum efficiency (α), PAR-saturated net photosynthetic rates (A_m), and the dark respiration rates (R_d) in equation (1) for

red mangrove foliage. The PAR compensation point was estimated as the PAR level at which A_N became zero.

$$A_N = \frac{\alpha \text{PAR}}{1 + (\alpha/[A_m + Rd])\text{PAR}} - R_d \qquad (1)$$

We also evaluated the appropriateness of the *Ball et al.* [1987] model (henceforth called the Ball-Berry model) for estimating g_{sv} in red mangroves. In this model g_{sv} is defined as a linear function of A_N, relative humidity (RH), and the leaf surface CO_2 mixing ratio (C_s) with slope m and b intercept as shown in equation (2). Leaf surface CO_2 mixing ratio is corrected for the CO_2 compensation point (Γ^*) to provide a better fit at low C_s values [*Leuning*, 1990].

$$g_{sv} = b + m\frac{A_n \text{RH}}{C_s - \Gamma^*} = b + m\Omega \qquad (2)$$

The A_N and g_{sv} models were applied separately to the three ensemble sets of leaf-level data, and correlation coefficients were used to evaluate their ability to capture the principal physiological attributes of mangrove foliage.

[10] Ab initio modifications to the Ball-Berry model were used to evaluate stomatal conductance values for mangrove foliage. In these modifications, the intercellular CO_2 mixing ratio (C_i, μmol mol^{-1}) was considered as an additional
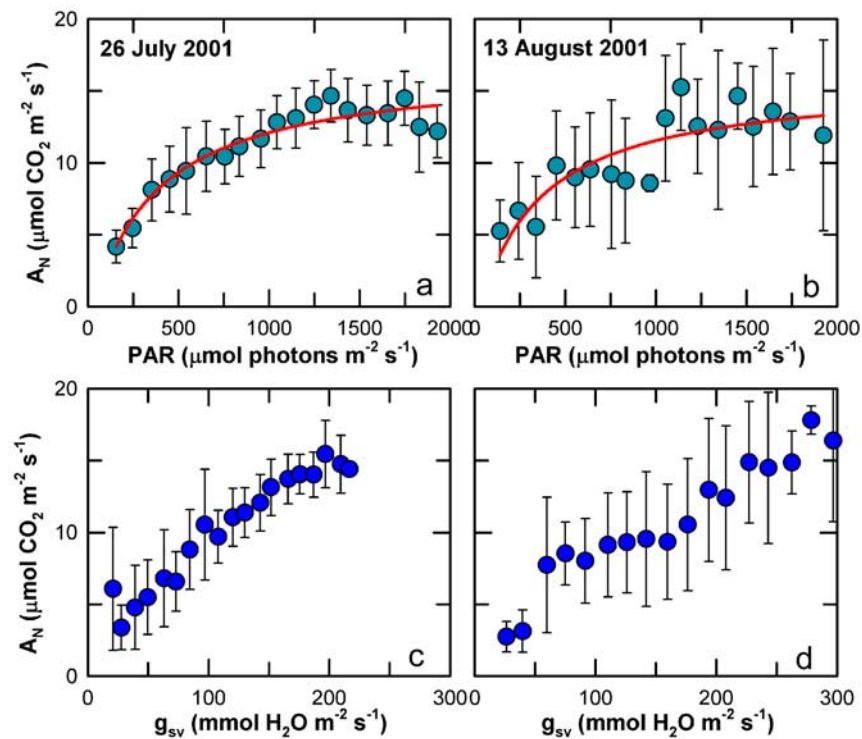
Figure 2. Relationship between net photosynthesis (A_N) and stomatal conductance to water vapor (g_{sv}) and response of A_N to (PAR) of tall red mangrove leaves under sunfleck conditions during (a and c) 26 July 2001 (n = 1162) and (b and d) 13 August 2001 (n = 781) at Key Largo. Error bars represent ± 1 standard deviation for each data bin. Figures 2a and 2c and Figures 2b and 2d include the same observations. Multivariate linear regression was used to produce the "best fit" line between A_n-PAR using equation (1).

forcing on g_{sv}. Values for C_i obtained during the leaf-level gas exchange measurements were multiplied by the Ball-Berry parameter (Ω) to produce the modified expression (equation (3)).

$$g_{sv} = b' + m'\frac{A_n RH}{C_s - \Gamma*}C_i = b' + m'\Omega C_i \qquad (3)$$

The slope (m') and intercept (b') for equation (3) were determined using least squares linear regression between measured g_{sv} values and the modified Ball-Berry parameter.

2.4. Maximum Rates of Carboxylation

[11] Maximum rates of carboxylation for mangroves are required as input to biospheric models designed to estimate carbon assimilation rates. Using the LI-6400 gas exchange system, we derived CO_2-A_N and PAR-A_N response curves on sunlit foliage at the Key Largo site. These data were used to derive the mean and standard deviations of the maximum rates of carboxylation ($V_{c\ max}$), PAR-limited carbon assimilation (J_{max}), and R_d for the *Farquhar et al.* [1980] biochemical model of photosynthesis. The CO_2-A_N response curves (n = 28) were generated using the following set points for CO_2 mixing ratios: 380, 330, 280, 230, 180, 130, 80, 30 μmole per mole. Set points for CO_2 were changed automatically in the cuvette when the coefficient of variation reached 1%. For these measurements leaf temperatures were maintained at 30°C and PAR was held at 1000 μmol photons m^{-2} s^{-1}. The PAR-A_N response curves (n =

19) were generated using the following set points for PAR: 2000, 1600, 1200, 1000, 800, 600, 400, 200, 100, 50, 20, 0 μmol photons m^{-2} s^{-1}. During these measurements, leaf temperature and CO_2 mixing ratios in the cuvette were held at 30°C and 380 μmol mol^{-1}, respectively. Leaves were allowed to equilibrate at each new PAR level before carbon assimilation measurements were made. To supplement the measurements at Key Largo, CO_2-A_N and PAR-A_N response curves were obtained at Watson River Chickee and at Little Rabbit Key. As described below, values for $V_{c\ max}$ and J_{max} derived from all field measurements were used to parameterize a model of canopy-level carbon fluxes.

2.5. Estimating Canopy-Level Carbon Fluxes

[12] The physiological attributes investigated during this study were incorporated in a canopy-level carbon assimilation model [*Barr*, 2005; *Gu et al.*, 1999]. Two versions of the canopy model were executed. One version included the original Ball-Berry stomatal conductance model (equation (2)) whereas the second version incorporated relationship (3). Using information obtained during 2004 on a 28-m tower located in the western Everglades [*Barr*, 2005], the model was driven by local climate variables such as solar irradiance, air temperature, specific humidity, and wind speed. It also included information regarding forest canopy architecture [*Barr*, 2005]. The multilayered model included the basic theory of the one reported by *Gu et al.* [1999], and contains modules for radiative transfer, coupled gas and energy exchange processes at the foliage level, and
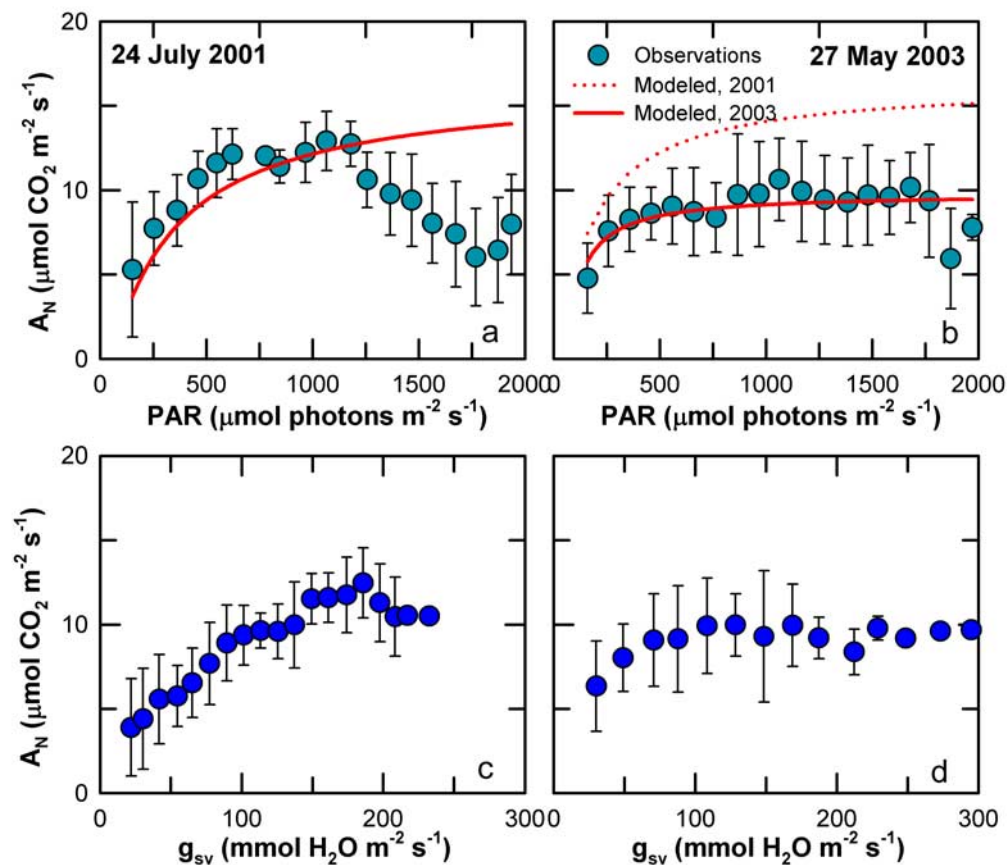
Figure 3. Relationship between net photosynthesis (A_N) and stomatal conductance to water vapor (g_{sv}) and response of A_N to (PAR) of tall red mangrove leaves exposed to direct irradiance throughout the day on (a and c) 24 July 2001 (n = 1123) and (b and d) 27 May 2003 (n = 1377) at Key Largo, Florida. The solid lines (Figures 3a and 3b) represent the Michaelis (equation (1)) model. Error bars represent ±1 standard deviation for each data bin.

turbulent transport. This work contains updated descriptions of atmospheric turbulence and diffusion within the canopy [*Barr*, 2005] as well as physiological attributes derived from the field data collected at our study sites. Also, ecosystem respiration was parameterized using an Arrhenius-type relationship [*Lloyd and Taylor*, 1994] between air temperature and above-canopy eddy covariance CO_2 fluxes determined during nighttime periods. Air temperature was selected as the control on nighttime respiration because of the better model fit that was obtained using air temperature rather than soil temperature. Separate functional relationships were derived during high tide when the soil surface was inundated and during low-tide periods when the soil surface was exposed. Net carbon ecosystem exchange between the 15-m tall mangrove forest and overlying atmosphere was estimated with the model at hourly intervals and the resulting carbon fluxes were integrated to produce monthly quantities.

3. Results

3.1. Leaf-Level Physiological Attributes

[13] On the tall fringing mangroves at the Key Largo site, exposed to variable light conditions, A_N increased hyperbolically with PAR levels, with maximum values on indi-

vidual leaves ranging from circa 12 to 18 μmol CO_2 m^{-2} s^{-1}. Ensemble-averaged quantities ranged from 16 to 18 μmol CO_2 m^{-2} s^{-1} (Figure 2). Maximum photosynthetic rates occurred predominantly during the morning hours under conditions of low VPD (<1.5 kPa). A_N at the Key Largo site reached irradiance saturation at PAR levels of $\sim$1200 ± 100 μmol m^{-2} s^{-1}. The resulting quantum efficiencies (α) ranged from 0.055 ± 0.01 to 0.071 ± 0.01 μmol CO_2 per μmol photons. The g_{sv} values on these leaves increased almost linearly with increasing A_N, similar to the results published by other authors [e.g., *Cheeseman and Lovelock*, 2004]. Maximum g_{sv} values reached $\sim$300 mmol H_2O m^{-2} s^{-1} and were measured on mangrove foliage under the influence of sunlit conditions in the early morning, and on leaves exposed to sunflecks and partial shading by the overlying canopy during the afternoon. The average rate of dark respiration for these leaves was estimated at 1.62 ± 1.32 μmol CO_2 m^{-2} s^{-1}.

[14] Red mangrove leaves exposed to continuous direct solar energy exhibited diurnal patterns of A_N and g_{sv} that were substantially different from leaves exposed to variable light conditions (Figure 3). On one of the sampling days (24 July 2001), A_N and g_{sv} values initially increased with PAR up to 1000 μmol m^{-2} s^{-1} but declined at higher levels. During a second sampling day (27 May 2003), the A_N and
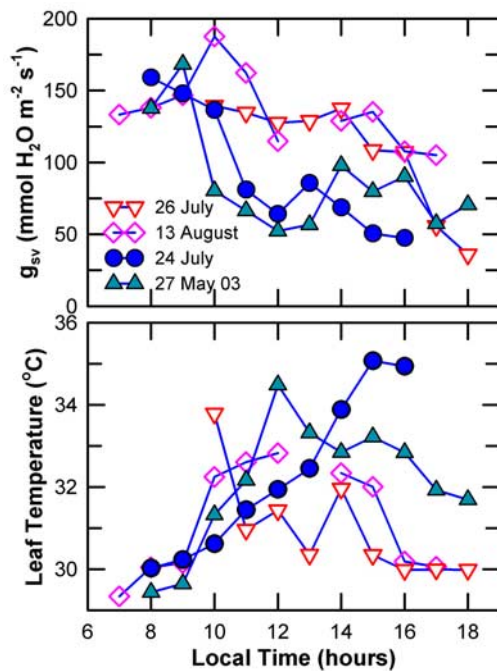
Figure 4. Daytime trends in leaf temperature (T_{leaf}) and stomatal conductance to water vapor (g_{sv}) of red mangrove leaves during 24 (circles), 26 July (inverted triangles), and 13 August (diamonds) 2001 and 27 May (triangles) 2003 at Key Largo, Florida. Points represent the mean of individual bins centered at uniform time intervals. The number of observations during 24 July, 26 July, 13 August, and 27 May is 1121, 1160, 784, and 1378, respectively. Solid symbols (24 July 2001 and 27 May 2003) represent sunlit leaves. Open symbols (26 July 2001 and 13 August 2001) represent leaves experiencing sunfleck conditions.

g_{sv} responses to increasing PAR levels were dampened in comparison to those observed on 24 July 2001. In general, the sunlit leaves on the exposed edges of the forest exhibited higher T_{leaf} and lower g_{sv} values than the sheltered leaves in the forest interior (Figure 4). Divergences in T_{leaf} and g_{sv} values in these two sets of leaves occurred around 10:00 h and increased throughout the day. Some recovery of g_{sv} was observed in sheltered leaves on all four sampling days after midday depressions at ~12:00 h and before the late afternoon declines.

[15] On average, the maximum rates of carbon assimilation for the dwarf variants at Taylor River reached $8–10$ μmol CO_2 m^{-2} s^{-1} (Figure 5), compared to $12–18$ μmol CO_2 m^{-2} s^{-1} observed in the tall fringe mangroves at the Key Largo site. Decreased photosynthesis in dwarf versus fringe red mangroves has been observed in other studies [e.g., *Cheeseman and Lovelock*, 2004]. The dwarf red mangrove foliage also displayed high variability in leaf level gas exchange rates on the three sampling days (19 July 2001, 20 May and 3 June 2003). Midday PAR values were sufficient (>1000 μmol m^{-2} s^{-1}) to achieve photosynthesis saturation on all three days and were not substantially different (Figure 5). At the Taylor River site, the predominant difference in environmental conditions was surface water salinity. The lowest A_N and g_{sv} values occurred on 19

July 2001 when the salinity was measured at 37 ‰. Higher A_N and g_{sv} values were observed on 20 May and 3 June 2003 when salinity was measured at 9‰ and 2‰, respectively.

[16] Water use efficiency was highest for the tall fringe mangroves with maximum values ranging from 100 to 150 μmol CO_2 per mmol H_2O during the morning hours (Figure 6). On average, dwarf mangroves had lower WUE values (~50 μmol CO_2 per mmol H_2O). Dwarf mangroves also exhibited lower LUE values compared to the tall fringe mangroves. The lowest LUE values in the dwarf mangroves occurred on 19 July 2001, corresponding to the period of highest salinities and relatively high WUE.

[17] For fully sunlit foliage at the Key Largo site, the ratio of mean J_{max} to mean $V_{c\ max}$ was 1.54. Average regression values derived for each of the CO_2-A_N and PAR-A_N response relationships for all leaves yielded maximum carboxylation and PAR-limited carbon assimilation rates of 76.1 ± 23.4 μmol CO_2 m^{-2} s^{-1} (n = 29) and 117 ± 41 μmol (e^-) m^{-2} s^{-1} (n = 19), respectively (Table 2).

[18] The relationship between A_N and C_i (Figure 7) was also investigated in the sheltered and exposed foliage. For sheltered foliage (Figure 7, top), A_N was correlated with C_i for $C_i < 225$ μmol mol^{-1}, as predicted from *Farquhar et al.*'s [1980] photosynthesis model. However, for all C_i values in the exposed foliage (Figure 7, bottom), A_N and C_i were uncorrelated. These results suggest complex pho-
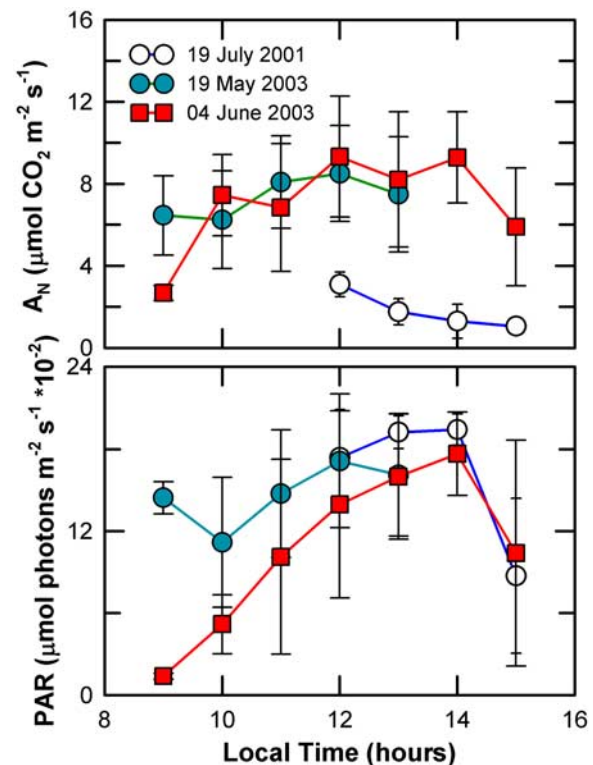
Figure 5. Midday trends in net photosynthesis (A_N) of dwarf red mangrove leaves and in situ photosynthetic active irradiance (PAR) during 19 July 2001 (n = 217), 19 May 2003 (n = 617), and 4 June 2003 (n = 1459) at Taylor River. Error bars for A_N and PAR represent ±1 standard deviation for each 1 h width bin centered on the hour.
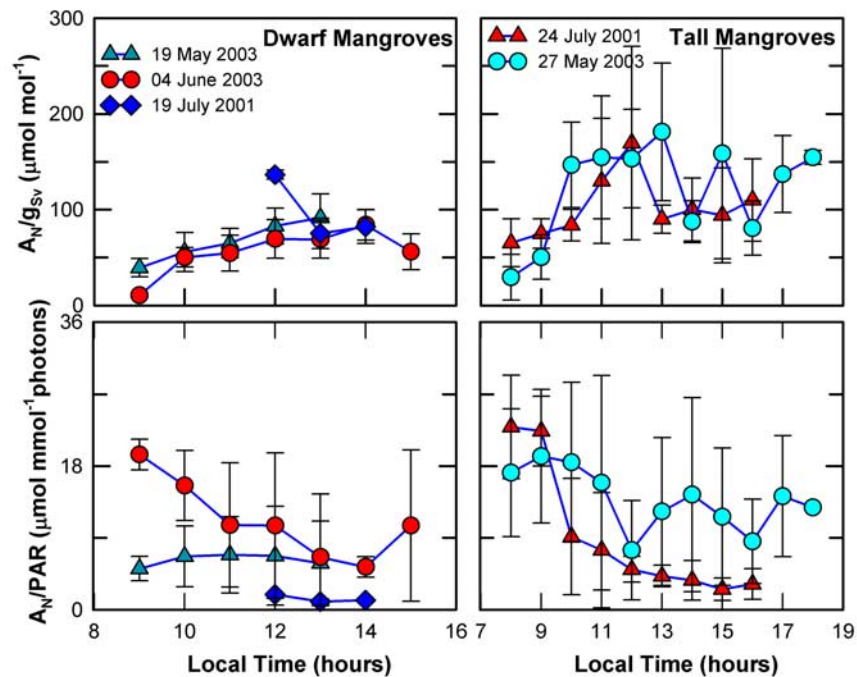
Figure 6. Measures of water use efficiency (A_N/g_{sv}) of dwarf red mangrove foliage at Taylor River during 19 July 2001 (diamonds), 19 May (diamonds), and 4 June (circles) 2003 and 'tall' red mangrove foliage during 24 July 2001 (triangles) and 27 May 2003 (circles) at Key Largo. The number of observations during 19 July, 19 May, 4 June, 24 July, and 27 May is 67, 601, 1420, 1117, and 1380, respectively. Error bars represent ±1 standard deviation for each 1 h width bin centered on the hour.

tosynthetic and stomatal responses to high irradiance and high temperature, and that standard leaf-level models relating A_N to C_i and g_{sv} may be inappropriate for mangroves in the Everglades environment.

3.2. Leaf-Level Models

[19] The interior-canopy foliage exhibited light responses which matched the Michaelis-type model (equation (1)), except at PAR values above 1500 μmol m^{-2} s^{-1} (Figure 2). This model was less successful in describing the light responses at all PAR levels among foliage that was continuously sunlit (Figure 3). Light responses were significantly different among the sheltered and exposed foliage, and exhibited significant variability between the 2001 and 2003 samplings, particularly in the south facing, sunlit leaves.

[20] The Ball-Berry model of stomatal conductance (equation (2)) showed variable levels of agreement with observations. The model captured the main features of stomatal conductance dynamics represented in the ensemble data collected on sheltered foliage at the Key Largo site from 26 July, 7 August, and 13 August 2001 (Table 1). As with the Michaelis-type model of A_N-PAR responses, the Ball-Berry model of stomatal conductance was less realistic in describing stomatal conductance in foliage exposed to direct solar irradiance throughout the day (Figure 8b). The model also showed less agreement with measurements at the Key Largo site compared to Taylor River. The reason for this discrepancy is unclear. However, multiplying the Ball-Berry parameter by C_i improved the level of agreement with g_{sv} observations at both sites. For example, when all days

(24 July, 26 July, 7 August, 13 August 2001, and 27 May 2003) of observations (n = 5075) for tall mangrove foliage at Key Largo were included, the modified algorithm in equation (3) reliably predicts stomatal conductance (r^2 = 0.98, Figure 8d and Table 1). The modified algorithm also captured much of the variance in g_{sv} observations (n = 2293) from the sunlit, exposed leaves from the dwarf mangroves at the Taylor River site (r^2 = 0.92, Figure 8c).

3.3. Seasonal Carbon Dioxide Assimilation Rates

[21] Modeled net carbon ecosystem exchange with the atmosphere exhibited seasonal variations, with maximum assimilation rates occurring during the spring (March to May) and fall (September to November), with minimum assimilation rates during June to August (Figure 9). These carbon assimilation trends resulted mostly from seasonal variations in solar irradiance, day length, and air temperature patterns. During the summer time, the mangrove forest canopy likely experienced the reduced physiological responses (Figure 4) due to elevated air temperatures. Also, nighttime ecosystem respiration rates were generally higher during summer months when air temperatures were highest (Table 3). However, the forest was inundated with water more frequently during summer months than at other times. These conditions partially suppressed respiration rates since the soil was covered with a layer of water. Therefore, only above ground components such as foliage and above ground pneumatophores contributed to ecosystem respiration.

[22] The original Ball-Berry module (equation (2)) included in the canopy model produced monthly carbon assimilation patterns that were markedly lower than the
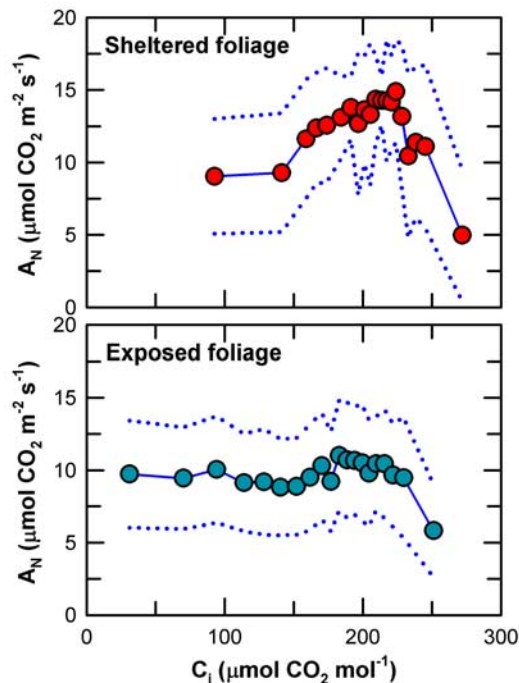
Figure 7. Relationship between net photosynthesis (A_N) and intercellular CO_2 mixing ratio (C_i). (top) Sheltered foliage included measurements on tagged tall red mangrove foliage at Key Largo on days 7 and 13 August 2001. (bottom) Exposed foliage included measurements on red mangrove foliage accessible from the water, including days 24 and 26 July 2001 and 27 May 2003. Only measurements where foliage was exposed to high PAR ($> = 1000$ μmol photons m^{-2} s^{-1}) were included. Twenty bins were created along C_i with an equal number of observations per bin. Dashed lines represent ±1 standard deviation for each bin.

modified Ball-Barry module (equation (3)). In fact, during June to September, the canopy model results with the original Ball-Barry module consistently yielded carbon fluxes as if the forest became a source of carbon. These carbon estimates were obtained when the forest experienced warm air masses whose monthly average air temperate exceeded 27°C. In contrast, the canopy model results with the modified Ball-Berry module showed carbon flux patterns that more closely followed the ones obtained from eddy covariance measurements [*Barr*, 2005] and revealed that the forest became a sink of carbon. Once integrated for the full season in 2004, the canopy model with the revised Ball and Berry module estimated that the mangrove forest consumed 870 gC per (m² year). This estimate favorably compared to the seasonal values derived from eddy covariance measurements (~917 gC per (m² year)). In contrast, using the traditional Ball-Barry module, the canopy model computed that the mangrove forest released 209 gC per (m² year) to the atmosphere.

4. Discussion

4.1. Mangrove Physiology and Climate

[23] The carbon assimilation patterns and stomatal dynamics (Figures 2 and 3) observed for *R. mangle* are different than those reported for mesophyte plants, but are similar to findings in other mangrove species [*Smith et al.*, 1989; *Björkman et al.*, 1988; *Cheeseman et al.*, 1991, 1997]. We also found $J_{max}/V_{c\,max}$ ratios were appreciably lower (1.54) than estimates for C_3 deciduous tree species. For example, *Wilson et al.* [2000] reported the ratio of mean J_{max} to mean $V_{c\,max}$ of 2.1 for deciduous tree species such as beech, red maple, black cherry, and tulip poplar in a closed forest in Oak Ridge, TN.

[24] We attribute these unusual physiological responses to two processes operating under high radiation loadings and high temperatures. First, red mangroves growing in saline environments must reduce stomatal opening to conserve water during periods when high evaporative demand exceeds the rate of salt exclusion/excretion and the supply of fresh water to the leaves. Second, the reduction in evaporative cooling caused by low g_{sv} results in foliage temperature exceeding 30°C and the partial deactivation of Photosystem II (Figure 4). For mangroves, photoinhibition and the deactivation of Photosystem II may represent irradiance-dependent carbon losses [*Ball and Passioura*, 1993; *Cheeseman et al.*, 1997]. This process may play a significant role in the overall carbon balance of these mangroves as foliage temperatures routinely exceed 30°C in the Florida Everglades.

[25] The morphological and physiological attributes of leaves in this study varied with their canopy position. For example, the exposed leaves facing south were more succulent than the sheltered leaves (data not shown). Evaporative cooling is less effective on these leaves due to their relatively high mass to leaf area ratio, and much of the energy absorbed by south facing foliage was converted into sensible heating. A_N and g_{sv} were consistently lower for the continuously sunlit than for sheltered foliage. These observations agree with *Smith et al.* [1989] who reported that PAR-saturated photosynthetic rates of *C. erectus* foliage were reduced by 50% during the cooler dry season compared to warm wet season measurements. *Smith et al.* [1989] argued that the reason for reduced carbon assimilation rates was due in part to the high soil salinities which caused a higher osmotic xylem potential and reduced stomatal conductance.

Table 1. Average and Associated Standard Deviation of Physiological Characteristics of Tall Red Mangroves at Key Largo With the Total Number of Observations Obtained While Foliage Temperature Was 30°C[a]

| Parameter	Average ± Standard Deviation	Number of Observations
V_{cmax} (μmol CO_2 m^{-2} s^{-1})	76.1 ± 23.4	29[b]
R_d (μmol CO_2 m^{-2} s^{-1})	1.62 ± 1.32	29[b]
J_{max} (μmol e$^-$ m^{-2} s^{-1})	117 ± 41	19[c]
q (μmol e$^-$ per (μmol photons^{-1})	0.43 ± 0.08	19[c]
θ	0.61 ± 0.33	19[c]
m[d]	2770 ± 303	2572
b[d]	45.5 ± 10.6	2572
m′[e]	26.4 ± 0.8	4718
b′[e]	18.1 ± 3.7	4718

[a]Model variables (see equations (2) and (3)) are also included.
[b]Value estimated based on sets of CO_2-A_N response relationships.
[c]Value estimated based on sets of PAR-A_N response relationships.
[d]See equation (2) for full definition of relationship.
[e]See equation (3) for full definition of relationship.
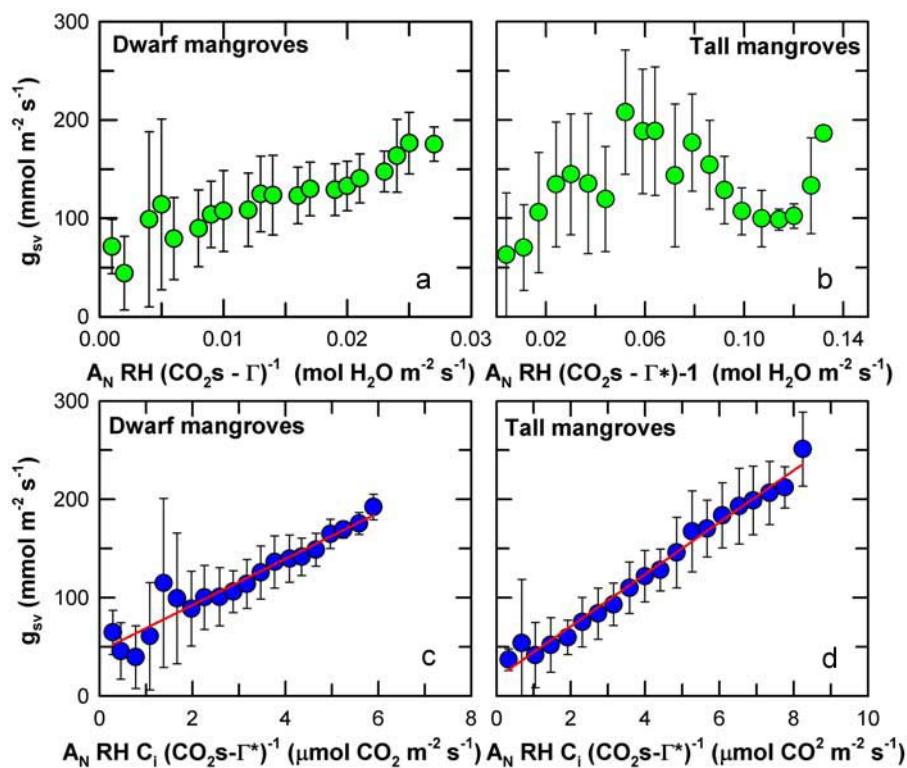
Figure 8. Relationship between stomatal conductance to water vapor (g_{sv}) and two parameters, (a and b) the Ball-Berry parameter (A_N RH $[CO_2s - \Gamma^*]^{-1}$) and (c and d) a new parameter (A_N RH C_i $[CO_2s - \Gamma^*]^{-1}$), for dwarf red mangroves at Taylor River including days 19 July 2001, 19 May 2003, and 4 June 2003, and for tall red mangroves at Key Largo including days 24 July, 26 July, 7 August, and 13 August 2001 and 27 May 2003. Separate best fit lines are included for the new model for each site. Observations (n = 4718) over the 5 days and observations (n = 2293) over 3 days are lumped in the analysis for Key Largo and Taylor River sites, respectively. Error bars represent ±1 standard deviation for each bin, where bins are evenly spaced along the x axis.

[26] Variations in *R. mangle* morphology and leaf-level physiology were also apparent across the nutrient and salinity gradients present in the Florida Everglades. In general, the dwarf variant exhibited lower maximum carboxylation rates compared to the tall (Figures 3 and 5). The dwarf red mangrove foliage also displayed significantly more variability in leaf-level gas exchange rates in response to the changes in the local environment. Short-term variability of net photosynthesis is ascribed to both physiological differences among leaves and to changes in climate forcings (e.g., PAR, temperature). Salinity may also have played a role, although we only have a few days of measurements to support this conclusion. The hypersaline conditions present during summer 2001 (maximum values of 37‰) were associated with lower xylem water potential (data not shown) and unusually low carbon assimilation rates less than 4 μmol CO_2 m^{-2} s^{-1} (Figure 5).

[27] Water use efficiencies measured on these leaves are comparable to previously published values for mangrove foliage in south Florida and throughout the tropics (Table 2; for the data included in Table 2, the WUE values were computed based on reported net photosynthesis and stomatal conductance). WUE can be an order of magnitude greater when plants experience salinity stress during the dry season [*Smith et al.*, 1989]. However, *Theuri et al.*

[1999] reported that severe salinity stress contributed to declines in WUE. We found WUE was highest for fringe mangroves in Key Largo during the morning hours before high solar irradiance levels and high temperatures contributed to reduced photosynthesis (Figure 6).

4.2. Leaf Level Models

[28] Over diurnal timescales, our measurements of carbon assimilation rates were similar to previously reported values for this species [*Lin and Sternberg*, 1992a, 1992b]. *Lugo et al.* [1975] reported maximum photosynthetic rates of ~12 μmol (CO_2) m^{-2} s^{-1} during August, and *Moore et al.* [1973] reported almost identical carbon assimilation rates for red mangroves on islands in Florida Bay during October. However, we found that the light response and stomatal dynamics in these trees could not be properly represented within the framework of leaf-level models such as those shown in (1) or (2), which hold only if increased radiational loads are at least partially offset by higher transpiration and thus greater evaporative cooling. Temperature is not explicitly represented in these models, and they assume there is no deactivation of Photosystem II or other changes in leaf physiological properties such as $V_{c\,max}$ and J_{max} with changes in radiational loadings. In contrast, our data show that leaf temperatures in mangrove foliage
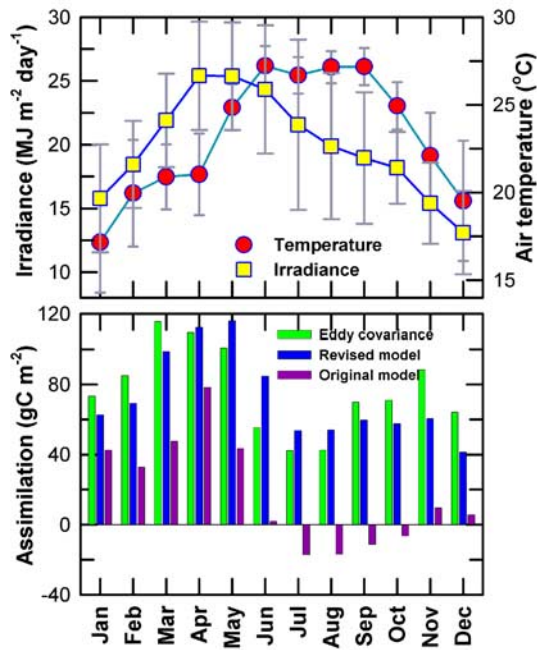
Figure 9. (top) Monthly sums of solar irradiance (circles) and average air temperature (squares). (bottom) Total monthly sum of modeled net carbon assimilation using both the revised and traditional stomatal conductance algorithms and monthly sum of measured CO_2 fluxes for the (tall) mangrove forest along Shark River in the Florida Everglades during the 2004 growing season.

routinely increase more than 3°C above air temperature as evaporative cooling decreases with g_{sv} under high irradiance. In general, we found that the traditional Michaelis-type PAR response model showed a closer correspondence to our observations in the sheltered compared to the sunlit, continuously exposed foliage, particularly at high irradiance.

[29] In the Florida Everglades, mangrove foliage exhibits the unique characteristic of conserving water loss through leaves by limiting stomatal opening with only moderate reductions in carboxylation. Even under the stresses of high temperature and high radiational loads, the mangrove foliage maintained C assimilation rates of circa $8-10$ μmol CO_2 m^{-2} s^{-1} (Figure 7, bottom). We also found that the relationship between g_{sv} and A_N in this foliage was variable and was reliably predicted by the standard Ball-Berry model only when conditioned on low PAR (<500 μmol m^{-2} s^{-1}) and for periods of low temperature and low VPD in the sheltered leaves. However, the inclusion of C_i as an additional forcing term (equation (3)) significantly improved the predictive ability of the Ball-Berry model when the relationship between A_N and g_{sv} did not follow typical patterns. For example, the C_i term improved the fit of the standard formulation during afternoon periods when PAR was high (>1000 μmol photons m^{-2} s^{-1}) and g_{sv} values declined at relatively constant A_N. The variable $g_{sv} - A_N$ relationships in this data set appear to have resulted from the ranges of environmental conditions and leaf physiological properties present within the canopy during sampling. The improvement in the Ball-Berry formulation results from the correlation between C_i and g_{sv}, which, in turn, reflects the control

of diffusion of atmospheric CO_2 into the mesophyll by stomata. C_i is also closely correlated with A_N over a wide range of conditions, since A_N is largely dependent on C_i [*Farquhar et al.*, 1980]. These interdependencies suggest A_N may be removed completely in favor of C_i in the modified expression. However, our data showed the relationship between A_N and C_i was also highly variable, and it was necessary to include both terms to produce the best overall fit with observed g_{sv}. For example, the data showed that for exposed foliage under PAR-saturating conditions, A_N and C_i were uncorrelated (Figure 7, bottom), and C_i was highly variable ranging from 60 to 250 μmol CO_2 mol^{-1}. On the other hand, for sheltered foliage (Figure 7, top) at Key Largo, A_N increased linearly with C_i between 90 to 225 μmol CO_2 mol^{-1} but decreased when C_i values increased above 225 μmol CO_2 mol^{-1}. We found that without A_N in the model, g_{sv} was correlated with the remaining terms [RH C_i (Cs-Γ*)$^{-1}$; a unitless number ranging from 0 to 1] only over the range 0.2 to 0.45 (data not shown). Furthermore, leaf g_{sv} values approached an asymptotic value for C_i above 150 and 175 mmol m^{-2} s^{-1}, and it was necessary to include A_N under these conditions to accurately represent our observations. Improvements in the standard Ball-Berry model were apparent with the inclusion of C_i even during low-stress periods when A_N and g_{sv} were positively correlated because it compensated for the variable $V_{c,max}$ values (and hence, the variable $A_N - g_{sv}$ relationships) exhibited in this ensemble data set.

[30] It is uncertain how well the stomatal conductance model, which was parameterized using summertime measurements, will perform during the winter dry season. However, we have some confidence that physiological characteristics do not change drastically across seasons based on follow up gas exchange measurements made during 5 March and 5 April 2004 along Shark River in the western Everglades. During this period, we found J_{max} values of 69.2 ± 25.1 and $V_{c,max}$ of 99.1 ± 35.8, which were similar to the values determined for the Key Largo mangroves during the summer of 2001 and 2003. The slope (m′, 20.6 ± 1.2) and the intercept (b′, 23.5 ± 4.1) of the relationship between observed g_{sv} and modified Ball-Berry parameter using data from Shark River did not change from the Key Largo results. We do not have leaf-level data during the relatively much lower temperatures that occur with the passage of cold fronts through this region, usually between December and February. Cold fronts are fairly short-lived in south Florida, but leaf physiological responses during these periods are expected to be the most different from summertime measurements. The lack of data during these periods limits the conclusions we can draw regarding the predictive ability of the revised conductance model in climatic conditions other than those in which it was developed.

4.3. Net Ecosystem Exchange of CO_2 and Canopy Models

[31] Canopy model estimates of net carbon assimilation by the mangrove forest (labeled 'Flux Tower' in Figure 1) along Shark River exhibited strong seasonal variations (Figure 9), and the two physiology modules included in the canopy model yielded divergent results. At the flux tower site, maximum carbon assimilation rates occurred during the spring (March–May) followed by a decline

Table 2. Water Use Efficiencies Reported or Calculated for Mangrove Foliage in South Florida, South America, Australia, and Africa

Mangrove Species	Field Site[a]	WUE (A_N/g_{sv}) (μmol CO_2 per mmol H_2O)	Reference
A. germinans, *L. racemosa,* and *R. mangle* seedlings	seedlings from Florida	35–90	*Pezeshki et al.* [1990]
R. mangle and *L. racemosa* adults	southwestern Florida	10–30	*Martin and Loeschen* [1993]
A. germinans, *L. racemosa,* and *R. mangle* adults	Venezuela	40–65	*Sobrado* [2000]
R. mangle adults	south Florida	40–55	*Lin and Sternberg* [1992a]
A. germinans, *L. racemosa,* *R. mangle,* and *C. erectus* adults	south Florida	35–40	*Snedaker and Araújo* [1998]
P. rhizophoreae propagules	Columbia	75	*Naidoo and von Willert* [1995]
A. germinans and *C. erectus*	Venezuela	10–100[b]	*Smith et al.* [1989]
A. germinans seedlings	South America	100–130	*Naidoo and von Willert* [1995]
Aegialitis annulata and *Aegiceras corniculatum* seedlings	Australia	60–100	
Ensemble of 19 adult species Families include Acanthaceae, Avicenniaceae, Euphorbiaceae, Meliaceae, Myrsinaceae, Plumbaginaceae, Rhizophoraceae, Sterculiaceae	eastern Australia, Paupa New Guinea	50–125	*Clough and Sim* [1989]
R. Stylosa adults	North Queensland, Australia	80–135	*Andrews and Muller* [1985]
Bruguiera parviflora and *B. gymnorrhizan* adults	North Queensland, Australia	40–100	*Cheeseman et al.* [1991]
A. marina adults	New South Wales, Australia	60–80[c]	*Sobrado and Ball* [1999]
B. gymnorrhiza and *A. marina* adults	South Africa	50–90	*Naidoo et al.* [1998]
R. mucronata and *C. tagal* adults	Kenya	50–100[d]	*Theuri et al.* [1999]

[a]For seedlings, the origin of the plant is listed. Plants are grown in greenhouses at different locations.
[b]Water use efficiency (WUE) was as low as 10 and as high as 100 during the wet and dry seasons, respectively.
[c]WUE was ~60 and ~80 when plants were exposed to seawater and hypersaline water.
[d]WUE was ~50 during the dry season and ~100 during the wet season.

during summer (June–August) and partial recovery during the fall season (October–November). Atmospheric conditions such as solar irradiance, day length, and air temperature patterns were most favorable during March through May when levels of midday solar irradiance were sufficient to promote near optimal foliage carboxylation rates. Additionally, during spring and fall seasons low monthly average air temperatures contributed to suppressed foliage respiration, especially during cool nighttime and early morning periods. The canopy model, which utilized the revised Ball-Berry stomatal conductance algorithm, captured seasonal trends in C assimilation, but underestimated assimilation rates during December through April. This result may be attributed to foliage acclimation to lower dry season temperatures which was not represented in the leaf-level subroutines in the canopy model. The leaf functions in this model were parameterized using data collected in the summertime, and the temperature responses of physiological attributes determined during this period were extrapolated to represent all seasons. During December and January, nighttime foliage respiration was lowest but day length and amount of solar irradiance limited foliage carbon assimilation.

[32] Beginning in June, the wet season commences in the Everglades, resulting in frequent afternoon thunderstorms and cloudy conditions, and a steady decline in the levels of direct solar irradiance that extends through September (Figure 9). During these months, the modeled net carbon ecosystem exchange only reached 5 μmol CO_2 m^{-2} s^{-1}. Under clear-sky conditions in the summer, high leaf temperatures and increased foliage respiration rates resulted in suboptimal leaf carboxylation rates and reduced net assimilation. Also, nighttime ecosystem respiration rates were greater during the summer months in response to higher air temperatures. Respiration may be mostly attributed to foliage, above ground roots, and biomass rather than soil. In comparing ecosystem respiration during inundated versus exposed soil conditions, respiration was only reduced by 0.63 μmol CO_2 m^{-2} s^{-1} on average (Table 3) when the soil was prevented from contributing to the measured CO_2 flux by a layer of water. When air temperatures exceeded ~30°C the temperature-induced photosynthetic deactivation also contributed to lower carbon assimilation rates. The deactivation routines employed in the model tended to overestimate the temperature effect, particularly during midday under clear skies, and this offset contributed to lower monthly C assimilation rates during July and August. In general, the revised Ball-Berry conductance algorithm more realistically captured midday stomatal dynamics compared to results using the traditional formulation (Figure 9).

5. Summary and Conclusions

[33] The synoptic mangrove physiological measurements made in the Florida Everglades allow for several conclu-

Table 3. Summary of Ecosystem Respiration and Arrhenius-Type Fit Characteristics When the Soil Surface Was Inundated During High Tide and When the Soil Surface Was Exposed to the Atmosphere During Low Tide[a]

Summary Characteristic	Exposed Soil Conditions (Low Tide)	Inundated Soil Conditions (High Tide)
Number of half-hourly periods	3579	2274
$\Sigma\ F_{RE}$ (g C m^{-2})	423	222
Mean F_{RE} (μmol m^{-2} s^{-1})	3.65	3.02
Mean air temperature ($^\circ$C)	20.5	21.6
$F_{RE,\ 10\ C}$[b] (μmol m^{-2} s^{-1})	2.28	1.74
E_a/R[b] (K)	3625	3870
R^2[b]	0.605	0.415

[a]Ecosystem respiration at 10 C ($F_{RE,10C}$) and the ratio of apparent activation energy to ideal gas constant (E_a/R (in kelvins)) were determined by nonlinear regression of binned CO_2 fluxes measured above the canopy. Thirty bins of CO_2 fluxes were constructed during both high- and low-tide conditions, and fluxes were sorted by air temperature with an equal number of observations per bin.

[b]The Arrhenius type fit [*Lloyd and Taylor*, 1994] of ecosystem respiration (F_{RE}) to air temperature (T_K (in kelvins)) was used with the following form: $F_{RE} = F_{RE,10C}\ \exp\left[\frac{E_a}{R}\ (1/283K - 1/T_K)\right]$.

sions. First, mangrove physiological attributes (e.g., J_{max} and $V_{c\ max}$) are unique, with $J_{max}/V_{c\ max}$ ratios (1.54) lower than deciduous tree species. As demonstrated in the application of a canopy model, the J_{max} and $V_{c\ max}$ data (Table 1) reported here must be included in ecophysiological models of the mangrove ecosystem. Second, elevated solar irradiance loadings (where PAR > 1000 μmol photons m^{-2} s^{-1}) routinely heat mangrove leaves above 33°C, thereby producing measurable reductions in foliage CO_2 assimilation rates. Third, based on field observations and model analyses we conclude that current ecophysiological models need to be modified to consider the influences of gradient regulators such as high salinity levels and elevated solar irradiance loadings (>500 W m^{-2} or ~1000 μmol photons m^{-2} s^{-1} of PAR) on the physiological responses of mangroves. As an interim approach, we propose a modified expression of the traditional Ball-Berry relationship to simultaneously estimate stomatal conductance and carbon assimilation in mangrove leaves. In hypersaline environments (>35‰), mangrove foliage experiences suppressed carbon assimilation rates and stomatal conductance. In part, these observed physiological responses are likely due to the inability of the mangroves growing in a saline environment to process the necessary fresh water to meet the prevailing evaporative demand. Fourth, on the basis of foliage physiological measurements and canopy modeling studies we conclude that tall red mangrove forests in Florida Everglades exhibit dynamic carbon assimilation patterns strongly modulated by the prevailing atmospheric conditions, and the physiological responses to the local climate identified in this study.

References

Alongi, D. M. (2008), Mangrove forests: Resilience, protection from tsunamis, and responses to global climate change, *Estuarine Coastal Shelf Sci.*, 76, 1–13.

Andrews, T. J., and G. J. Muller (1985), Photosynthetic gas exchange of the mangrove, Rhizophora stylosa Griff. in its natural environment, *Oecologia*, 65, 449–455.

Ball, J. T., I. E. Woodrow, and J. A. Berry (1987), A model predicting stomatal conductance and its contribution to the control of photosynthesis under different environmental conditions, in *Progress in Photosynthesis Research*, vol. 4, edited by I. Biggins, pp. 221–224, Martinus-Nijhoff, Dordrecht, Netherlands.

Ball, M. C. (1986), Photosynthesis in mangroves, *Wetlands (Australia)*, 6, 12–22.

Ball, M. C., and J. Passioura (1993), Carbon gain in relation to water use: Photosynthesis in mangroves, in *Ecophysiology of Photosynthesis*, edited by E. Schulze and M. M. Caldwell, pp. 47–59, Springer, Berlin.

Ball, M. C., I. R. Cowan, and G. D. Farquhar (1988), Maintenance of leaf temperature and the optimisation of carbon gain in relation to water loss in a tropical mangrove forest, *Aust. J. Plant Physiol.*, 15, 263–276.

Barr, J. G. (2005), Carbon sequestration by riverine mangroves in the Florida Everglades, Ph.D. dissertation, 183 pp., Dep. of Environ. Sci., Univ. of Va., Charlottesville.

Björkman, O., B. Demmig, and T. J. Andrews (1988), Mangrove photosynthesis: Response to high-irradiance stress, *Aust. J. Plant Physiol.*, 15, 43–61.

Bouillon, S., et al. (2008), Mangrove production and carbon sinks: A revision of global budget estimates, *Global Biogeochem. Cycles*, 22, GB2013, doi:10.1029/2007GB003052.

Cheeseman, J. M., and C. E. Lovelock (2004), Photosynthetic characteristics of dwarf and fringe Rhizophora mangle L. in a Belizean mangrove, *Plant Cell Environ.*, 27, 769–780.

Cheeseman, J. M., B. F. Clough, D. R. Carter, C. E. Lovelock, J. E. Ong, and R. G. Sim (1991), The analysis of photosynthetic performance in leaves under field conditions: A case study using Bruguiera mangroves, *Photosynth. Res.*, 29, 11–22.

Cheeseman, J. M., L. B. Herendeen, J. M. Cheeseman, and B. F. Clough (1997), Photosynthesis and photorespiration in mangroves under field conditions, *Plant Cell Environ.*, 20, 579–588.

Clough, B. F., and R. G. Sim (1989), Changes in gas exchange characteristics and water use efficiency of mangroves in response to salinity and vapor pressure deficit, *Oecologia*, 79, 38–44.

Dwyer, L. M., and D. W. Stewart (1986), Effect of leaf age and position on net photosynthetic rates in maize (Zea mays L.), *Agric. For. Meteorol.*, 37, 29–46.

Farquhar, G. D., S. von Caemmerer, and J. A. Berry (1980), A biochemical model of photosynthetic CO_2 assimilation in leaves of C$_3$ species, *Planta*, 149, 78–90.

Fuentes, J. D., and K. M. King (1989), Leaf photosynthesis and leaf conductance of maize grown hydroponically and in soil under field conditions, *Agric. For. Meteorol.*, 45, 155–166.

Gu, L., H. H. Shugart, J. D. Fuentes, T. A. Black, and S. R. Shewchuk (1999), Micrometeorology, biophysical exchanges and NEE decomposition in a two-story boreal forest—Development and test of an integrated model, *Agric. For. Meteorol.*, 94, 123–148.

Koch, M. S., and S. C. Snedaker (1997), Factor influencing Rhizophora mangle L. seedling development in Everglades carbnonatae soils, *Aquat. Bot.*, 59, 87–98.

Leuning, R. (1990), Modeling stomatal behavior and photosynthesis of Eucalyptus gandis, *Aust. J. Plant Physiol.*, 17, 159–175.

Lin, G., and L. D. S. L. Sternberg (1992a), Comparative study of water uptake and photosynthetic gas exchange between scrub and fringe red mangroves, Rhizophora mangle L, *Oecologia*, 90, 399–403.

Lin, G., and L. D. S. L. Sternberg (1992b), Effect of growth form, salinity, nutrient and sulfide on photosynthesis, carbon isotope discrimination and growth of Red mangrove (Rhizophora mangle L.), *Aust. J. Plant Physiol.*, 19, 509–517.

Lloyd, J., and J. A. Taylor (1994), On the temperature dependence of soil respiration, *Funct. Ecol.*, 8, 315–323.

Lugo, A. E., and S. C. Snedaker (1974), The ecology of mangroves, *Annu. Rev. Ecol. Syst.*, 5, 39–64.

Lugo, A. E., G. Evink, M. M. Brinson, A. Broce, and S. C. Snedaker (1975), Diurnal rates of photosynthesis, respiration, and transpiration in mangrove forests of south Florida, in *Tropical Ecological Systems Trends in Terrestrial and Aquatic Research*, edited by F. B. Golley and E. Medina, pp. 335–350, Springer, New York.

Martin, C. E., and V. S. Loeschen (1993), Photosynthesis in the mangrove species Rhizophora mangle L.: No evidence for CAM-cycling, *Photosynthetica*, 28, 391–400.

Mitsch, W. J., and J. G. Gosselink (2000), The value of wetlands: Importance of scale and landscape setting, *Ecol. Econ.*, *35*, 25–33.

Moore, R. T., P. C. Miller, J. Ehleringer, and W. Lawrence (1973), Seasonal trends in gas exchange characteristics of three mangrove species, *Photosynthetica*, *7*, 387–394.

Naidoo, G., and D. J. von Willert (1995), Diurnal gas exchange characteristics and water use efficiency of three salt-secreting mangroves at low and high salinities, *Hydrobiologia*, *295*, 13–22.

Naidoo, G., H. Rogalla, and D. J. von Willert (1998), Field measurements of gas exchange in *Avicennia marina* and *Bruguiera gymnorrhiza*, *Mangroves Salt Marshes*, *2*, 99–107.

Pezeshki, S. R., R. D. DeLuane, and W. H. Patrick Jr. (1990), Differential response of selected mangroves to soil flooding and salinity: Gas exchange and biomass partitioning, *Can. J. For. Res.*, *20*, 869–874.

Robertson, A. I., and D. M. Alongi (1992), *Tropical Mangrove Ecosystems*, 329 pp., AGU, Washington, D. C.

Smith, J. A. C., et al. (1989), Ecophysiology of xerophytic and halophytic vegetation of a coastal alluvial plain in northern Venezuela. VI. Water relations and gas exchange of mangroves, *New Phytol.*, *111*, 293–307.

Smith, T. J., III, M. B. Robblee, H. R. Wanless, and T. W. Doyle (1994), Mangroves, hurricanes, and lightning strikes, *BioScience*, *44*, 256–262.

Snedaker, S. C., and R. J. Araújo (1998), Stomatal conductance and gas exchange in four species of Caribbean mangroves exposed to ambient and increased CO_2, *Mar. Freshwater Res.*, *49*, 325–327.

Sobrado, M. A. (2000), Relation of water transport to leaf gas exchange properties in three mangrove species, *Trees (Berl.)*, *14*, 258–262.

Sobrado, M. A., and M. C. Ball (1999), Light use in relation to carbon gain in the mangrove, *Avicennia marina*, under hypersaline conditions, *Aust. J. Plant Physiol.*, *26*, 245–251.

Theuri, M. M., J. I. Kinyamario, and D. van Speybroeck (1999), Photosynthesis and related physiological processes in two mangrove species, *Rhizophora mucronata* and *Ceriops tagal*, at Gazi Bay, Kenya, *Afr. J. Ecol.*, *37*, 180–193.

Twilley, R. R., R. H. Chen, and T. Hargis (1992), Carbon sinks in mangroves and their implications to carbon budget of tropical coastal ecosystems, *Water Air Soil Pollut.*, *64*, 265–288.

Valiela, I., J. L. Bowen, and J. K. York (2001), Mangrove forests: One of the world's threatened major tropical environments, *BioScience*, *51*, 807–881.

Ward, G. A., T. J. Smith, K. R. T. Whelan, and T. W. Doyle (2006), Regional processes in mangrove ecosystems: Spatial scaling relationships, biomass, and turnover rates following catastrophic disturbance, *Hydrobiologia*, *567*, 517–527.

Wilson, K., D. D. Baldocchi, and P. J. Hanson (2000), Spatial and seasonal variability of photosynthetic parameters and their relationship to leaf nitrogen in a deciduous forest, *Tree Physiol.*, *20*, 565–578.

————————————

J. G. Barr, J. D. Fuentes, and J. C. Zieman, Department of Environmental Sciences, University of Virginia, Charlottesville, VA 22904, USA. (jf6s@virginia.edu)

V. Engel, Everglades National Park, Homestead, FL 33030, USA.